JOURNAL OF GUIDANCE, CONTROL, AND DYNAMICS
Vol. 25, No. 4, July–August 2002

Optimal Near-Minimum-Time Control Design for Flexible Structures

Bassam A. Albassam*
King Saud University, Riyadh 11421, Saudi Arabia

A method for generating a near-minimum-time control input for flexible structures is presented with the objective of minimizing the maneuver time and the residual energy of the flexible modes. The method is based on smoothing the bang–bang, time-optimal control input designed for the rigid-body mode. Smoothing is accomplished through the addition, to the basic time-optimal control problem for the rigid-body mode, of a constraint that limits the first time derivative for the resulting control input. If the first time-derivative constraint is replaced with the second time-derivative constraint, then smoother control input is generated. The necessary conditions of optimality for the resulting time-optimal control problem, with control and state constraints, are derived, which leads to forming a boundary-value problem. The resulting boundary-value problem is solved using the shooting method. The capability of this method is demonstrated through a numerical example in which the smooth control input is able to eliminate the residual energy of the flexible modes at the expense of a slight increase in maneuver time.

I. Introduction

In recent years there has been considerable interest in modeling and control of flexible structures. This is attributable to the use of lightweight materials to increase both speed and fuel efficiency. Furthermore, many applications, such as robotic manipulators, disc drive heads, and pointing systems in space, are required to maneuver as quickly as possible without significant structural vibrations during and/or after a maneuver.

The time-optimal control for general maneuvers and general flexible structures has posed a challenging problem and is still an open area for research. In particular, the time-optimal control for rest-to-rest slewing maneuvers of flexible structures has been an active area of research, and only limited solutions have been reported in the literature. Solution of the time-optimal control problem of a general flexible system has two main obstacles. First, the number of control switching times is unknown a priori and must be guessed. Second, as the number of modes included in the model is increased, the computer time required by these numerical techniques becomes prohibitive.

In the recent literature, many researchers[1–9] have developed computational techniques that deal with solving time-optimal control for flexible structures. In all of these published works, the exact time-optimal control input, which is of the bang–bang type, is calculated. From an implementation point of view, the bang–bang type of control can easily excite the higher-order modes that are neglected in the model. Junkins et al.[10] and Hecht and Junkins[11] have used an approximation function for the bang–bang control input with the objective of eliminating the sudden change of control magnitudes at a switching time, resulting in a smoother control input.

This paper is concerned with the design of a near-minimum-time control input for a flexible structure with one rigid-body mode and many flexible modes to perform a desired rest-to-rest maneuver. The basic idea behind the approach is to smooth the bang–bang, time-optimal control input calculated for the rigid-body mode. A smooth control input without sharp transitions, when applied to a flexible structure, is less likely to excite the structural modes during maneuvers.

Presented as Paper 2000-4150 at the AIAA Guidance, Navigation, and Control Conference, Denver, CO, 14–17 August 2000; received 31 July 2001; revision received 14 March 2002; accepted for publication 22 March 2002.

*Assistant Professor, College of Engineering, Mechanical Engineering Department; albassam@ksu.edu.sa. Member AIAA.

A smoothed bang–bang control input is calculated by formulating and solving an optimal control problem with the objective of minimizing the maneuver time and subject to the state equations describing the rigid-body mode, boundary conditions, and an additional constraint that limits the first time derivative of the control input. A simple and novel numerical technique is developed that solves the resulting boundary-value problem derived as a result of applying the necessary conditions of optimality. In the next step, a smoother control input is calculated by formulating and solving a time-optimal control problem with the same objective, state equations, and boundary conditions, as the previous one, but replacing the additional constraint with one that limits the second time derivative of the control input. Finally, the resulting smooth control input is applied to the general flexible system with the aim of minimizing both the maneuver time as well as the free vibration at the end of the maneuver. The main difference between the proposed technique and that of Junkins et al.[10] and Hecht and Junkins[11] is that the type of smoothing function is automatically generated from the solution of the optimal control problem.

As an example to illustrate the numerical procedure, we consider the time-optimal single-axis rotation problem for a system consisting of a rigid hub with elastic appendages attached to it. A single actuator that exerts an external torque on the rigid hub controls the system. It is required to rotate the system by a certain angular displacement and in minimum time. A numerical simulation of the problem shows that the smooth control inputs, while achieving a near-minimum-time maneuver, significantly minimized the energy spillover to the flexible modes, thus resulting in excellent pointing accuracy.

II. Problem Formulation

Consider a general linear model of a flexible structure with one rigid-body mode and n flexible modes, which can be represented by the vector differential equations

$$M\ddot{\boldsymbol{x}} + C\dot{\boldsymbol{x}} + K\boldsymbol{x} = \boldsymbol{b}u \tag{1}$$

where $\boldsymbol{x} \in \Re^{n+1}$ is the generalized displacement vector and M, C, and K are the mass, damping, and stiffness matrices of appropriate dimensions, respectively. The vector $\boldsymbol{b} \in \Re^{n+1}$ is the control influence vector, and $u(t)$ is a scalar control input bounded as

$$-u_{\max} \le u(t) \le u_{\max} \tag{2}$$

It is desired to transfer the system in Eq. (1) from the initial conditions $\boldsymbol{x}(0) = [0\ 0\ 0\ \cdots\ 0]^T$ to the final conditions $\boldsymbol{x}(t_f) = [\boldsymbol{x}_{1f}\ 0\ 0\ \cdots\ 0]^T$ and subject to the control constraints [Eq. (2)] in minimum time.

The system in Eq. (1) can be transformed into the decoupled modal equations using the eigenvectors of the system to the form

$$\ddot{\theta} = \phi_0 u \tag{3}$$

$$\ddot{\boldsymbol{q}}_i + 2\sigma_i \dot{\boldsymbol{q}}_i + \omega_i^2 \boldsymbol{q}_i = \phi_i u, \qquad i = 1, \ldots, n \tag{4}$$

where $\theta(t)$ is the rigid-body coordinate, $\boldsymbol{q}_i(t)$ is the ith modal coordinate, and σ_i and ω_i are the ith damping factor and frequency, respectively. Scalars ϕ_i, $i = 0, \ldots, n$, are defined by

$$[\phi_0 \quad \phi_1 \quad \cdots \quad \phi_n]^T = \Phi^T \boldsymbol{b} \tag{5}$$

where Φ is the matrix of eigenvectors and superscript T denotes a transpose.

III. Time-Optimal Control Design for the Rigid-Body Mode

As a first step toward designing a smooth control input, we introduce the time-optimal control problem for the rigid-body mode [Eq. (3)] that results in a bang–bang type of control input. Writing a state-space model for Eq. (3) gives

$$\dot{\theta}_1 = \theta_2, \qquad \dot{\theta}_2 = \phi_0 u \tag{6}$$

where $\theta_1 = \theta$ and $\theta_2 = \dot{\theta}$ are, for example, the angular displacement and velocity, respectively.

The time-optimal control problem is to find the control input $u(t)$ that minimizes the objective function

$$J = \int_0^{tf} \mathrm{d}t = t_f \tag{7}$$

subject to the state equations [Eqs. (6)], the control constraints [Eqs. (2)], and the following boundary conditions:

$$\theta_1(0) = 0, \qquad \theta_1(t_f) = \theta_f, \qquad \theta_2(0) = 0, \qquad \theta_2(t_f) = 0 \tag{8}$$

where $\boldsymbol{x}_{1f}$ is transformed to θ_f using the matrix of eigenvectors Φ. An analytical solution to this problem can be found in Refs. 7 and 12, where the control input is bang–bang and contains at most one switch.

If this control input is applied to the system in Eq. (1), then, because of neglecting all of the flexible modes, a free vibration occurs at the end of the maneuver. This free vibration is a result of control spillover to these modes.[4] To minimize this free vibration, it is natural that we should eliminate the sharp transitions of the bang–bang control so that the energy transfer to the flexible modes is minimized.

IV. Time-Optimal Control Design for the Rigid-Body Mode with a First Time-Derivative Constraint

In this section, we formulate and solve a time-optimal control problem for the rigid-body mode that results in a smooth control input. A simple and novel idea would be to add, to the previous time-optimal control problem, a state variable describing the first time derivative of the control input along with an additional constraint that limits this derivative to a user-defined maximum. Consequently, the degree of smoothness of the generated control input is controlled through the maximum value of the control first time derivative.

Therefore, we consider the following time-optimal control problem: Determine the control input $u(t)$ that minimizes

$$J = \int_0^{tf} \mathrm{d}t = t_f \tag{7}$$

and subject to the state equations

$$\dot{\theta}_1 = \theta_2, \qquad \dot{\theta}_2 = \phi_0 u, \qquad \dot{u} = u_d \tag{9}$$

the state constraints

$$S_1 = u - u_{\max} \le 0, \qquad S_2 = -u - u_{\max} \le 0 \tag{10}$$

the control constraints

$$u_d - (u_d)_{\max} \le 0, \qquad -u_d - (u_d)_{\max} \le 0 \tag{11}$$

and the following boundary conditions:

$$\theta_1(0) = 0, \qquad \theta_1(t_f) = \theta_f, \qquad \theta_2(0) = 0$$
$$\theta_2(t_f) = 0, \qquad u(0) = 0, \qquad u(t_f) = 0 \tag{12}$$

Note that, in the preceding formulation, we consider $u(t)$ as an additional state variable and $u_d(t)$ as the control input. The reason for the addition of constraints, in Eqs. (11), is to replace the infinite time derivative of the bang–bang control input at a switching time with a finite magnitude that can not exceed $(u_d)_{\max}$. Consequently, the resulting time-optimal control problem contains both control constraints as well as state constraints. The numerical solution for this problem is based on the necessary conditions of optimality and is shown to satisfy a boundary-value problem.

A. Necessary Conditions of Optimality

The necessary conditions of optimality for general optimal control problems with control and state constraints are derived and discussed by Hamilton,[13] Maurer,[14] Maurer and Gillessen,[15] Oberle,[16] Maurer and Wiegand,[17] and Jacobson et al.,[18] among others. Following Jacobson et al.,[18] the necessary conditions of optimality are derived by defining first the Hamiltonian H as

$$H = 1 + \lambda_1 \dot{\theta}_1 + \lambda_2 \dot{\theta}_2 + \lambda_3 \dot{u} + \eta_1 (u - u_{\max}) + \eta_2 (-u - u_{\max})$$
$$= 1 + \lambda_1 \theta_2 + \lambda_2 \phi_0 u + \lambda_3 u_d + \eta_1 (u - u_{\max}) + \eta_2 (-u - u_{\max}) \tag{13}$$

where λ_i, $i = 1, \ldots, 3$, are the costates (Lagrange multipliers). The necessary conditions of optimality require the following equations to be satisfied:

1) State equations

$$\dot{\theta}_1 = \frac{\partial H}{\partial \lambda_1} \Rightarrow \dot{\theta}_1 = \theta_2, \qquad \dot{\theta}_2 = \frac{\partial H}{\partial \lambda_2} \Rightarrow \dot{\theta}_2 = \phi_0 u$$
$$\dot{u} = \frac{\partial H}{\partial \lambda_3} \Rightarrow \dot{u} = u_d \tag{9}$$

2) Costate equations

$$\dot{\lambda}_1 = -\frac{\partial H}{\partial \theta_1} \Rightarrow \dot{\lambda}_1 = 0, \qquad \dot{\lambda}_2 = -\frac{\partial H}{\partial \theta_2} \Rightarrow \dot{\lambda}_2 = -\lambda_1$$
$$\dot{\lambda}_3 = -\frac{\partial H}{\partial u} \Rightarrow \dot{\lambda}_3 = -\phi_0 \lambda_2 - \eta_1 + \eta_2 \tag{14}$$

where $\eta_1(t)$ and $\eta_2(t)$ are multiplier functions that satisfy

$$\eta_1 (u - u_{\max}) = 0, \qquad \eta_2 (-u - u_{\max}) = 0 \tag{15a}$$

where

$$\eta_1(t) = \begin{cases} 0 & \text{if} \quad u - u_{\max} < 0 \\ \ge 0 & \text{if} \quad u - u_{\max} = 0 \end{cases}$$

$$\eta_2(t) = \begin{cases} 0 & \text{if} \quad -u - u_{\max} < 0 \\ \ge 0 & \text{if} \quad -u - u_{\max} = 0 \end{cases} \tag{15b}$$

3) The time-optimal control $u_d^*(t)$. A subarc of $u(t)$ for which all of the state constraints are not active, that is, $S_i(u(t)) < 0$, is called an interior arc, whereas a boundary arc is a subarc of $u(t)$ when one of the state constraints is active, that is, $S_i(u(t)) = 0$, $i = 1$ or 2.

a) For an interior arc ($u - u_{\max} < 0$ and $-u - u_{\max} < 0$), the time-optimal control $u_d^*(t)$ must satisfy

$$u_d^*(t) = -(u_d)_{\max} \operatorname{sign}\left(\frac{\partial H}{\partial u_d}\right) \Rightarrow u_d^*(t) = -(u_d)_{\max} \operatorname{sign}(\lambda_3(t)) \tag{16}$$

Therefore, the costate variable $\lambda_3(t)$ is the switching function.

b) For a boundary arc $[u(t) - u_{\max} = 0$ or $-u(t) - u_{\max} = 0]$, the time-optimal control $u_d^*(t)$ is derived from

$$\dot{S}_i = 0, \qquad i = 1, \ldots, 2, \qquad \Rightarrow \dot{u}(t) = 0 \Rightarrow u_d^*(t) = 0 \quad (17)$$

$$\frac{\partial H}{\partial u_d} = 0 \Rightarrow \lambda_3(t) = 0 \quad (18)$$

4) The transversality condition for the free end time t_f yields

$$H(t) = 0, \qquad 0 \le t \le t_f \quad (19)$$

5) The boundary conditions that are given in Eqs. (12).

In general, a costate variable that is associated with state constraints, in this case $\lambda_3(t)$, may become discontinuous when any of the state constraints becomes active. However, the other costates, $\lambda_1(t)$ and $\lambda_2(t)$, are associated with states that are not constrained, and, hence, they are continuous. Furthermore, a constraint is said to be of order p if the pth time derivative of the constraints S_i in Eq. (10) is the first to contain the control variable $u_d(t)$ explicitly. In this case, it is easy to prove that p is equal to one. Maurer[14] has derived the necessary conditions for the optimality of junctions between interior and boundary arcs for a control variable appearing linearly in the equations of motion. In the same study, he proved that, under certain conditions, namely, if $p = 1$ and the boundary control as determined by Eq. (17) is less than $(u_d)_{\max}$, the costate $\lambda_3(t)$ is continuous (not necessarily continuously differentiable). The costate $\lambda_3(t)$ being continuous greatly simplifies the numerical algorithm to search for the optimal solution.

To reduce the numerical complexity to search for the optimal solution, we proceed in two steps. First, a solution in state space is guessed, which dispenses with the costates λ_1, λ_2, and λ_3. This type of solution leans on the special feature[17] that the optimal control structure contains as many free parameters as there are interior and boundary conditions for the state variables θ_1, θ_2, and u. Second, the costate variables are calculated using the state-space solution.

The state-space solution can be guessed by, first, solving the preceding optimal control problem without imposing the state constraints [Eqs. (10)], which leads to an optimal control problem with only control constraints. The necessary conditions of optimality for this problem can be found in Refs. 7 and 12, where the control structure will be of the bang–bang type with a maximum of two control switches.

Therefore, when the state constraints [Eqs. (10)] are included in the optimal control problem, the variables $u_d(t)$ and $u(t)$ should have the structures shown in Fig. 1, where t_{si} is the ith switching time and t_f is the final time.

Consequently, the solution, for the constrained optimal control problem in state space, consists of solving the boundary-value problem with the eight variables θ_1, θ_2, u, t_{s1}, t_{s2}, t_{s3}, t_{s4}, and t_f.

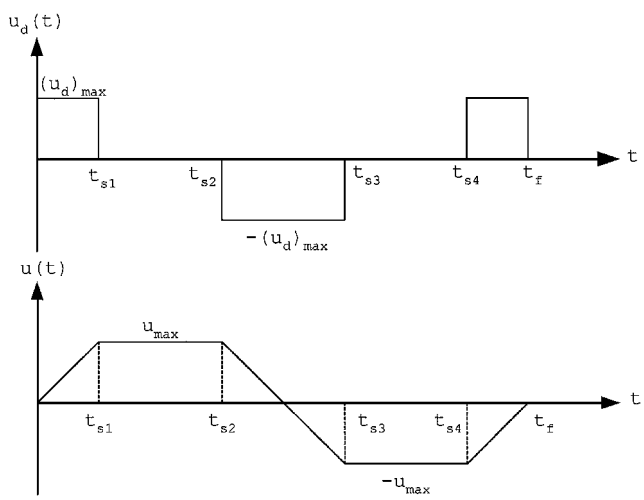

Fig. 1 Constrained time-optimal structure for $u_d(t)$ and $u(t)$.

On the other hand, the boundary and interior conditions consists of the six boundary conditions [Eqs. (12)], and the following two interior conditions, which are deduced from Fig. 1:

$$u(t_{s1}) = u_{\max}, \qquad u(t_{s3}) = -u_{\max} \quad (20)$$

B. Numerical Algorithm

Several numerical techniques[14–16] can be used to solve the derived boundary-value problem. In this paper, a simple numerical technique is proposed that is based on the simple shooting method. The numerical procedure is illustrated in the following steps.

1) Assume starting values for the switching and final times t_{s1}, t_{s2}, t_{s3}, t_{s4}, and t_f.

2) Integrate the state equations [Eqs. (9)], using the initial conditions in Eqs. (12), the control structure for $u_d(t)$ shown in Fig. 1, and the assumed or updated values for the switching and final times.

3) Form the vector of errors

$$\boldsymbol{f} = \begin{Bmatrix} \theta_1(t_f) - \theta_f \\ \theta_2(t_f) \\ u(t_f) \\ u(t_{s1}) - u_{\max} \\ u(t_{s3}) + u_{\max} \end{Bmatrix} \quad (21)$$

This vector is formed so that, when all of the components of $\boldsymbol{f}$ are equal to zeros, the boundary and interior conditions [Eqs. (12) and (20)] are satisfied, and we hope we have reached an optimal solution.

4) Calculate the Jacobian matrix

$$\frac{\partial \boldsymbol{f}}{\partial \boldsymbol{g}} = \begin{bmatrix} \frac{\partial f_1}{\partial t_{s1}} & \frac{\partial f_1}{\partial t_{s2}} & \frac{\partial f_1}{\partial t_{s3}} & \frac{\partial f_1}{\partial t_{s4}} & \frac{\partial f_1}{\partial t_f} \\ \frac{\partial f_2}{\partial t_{s1}} & \frac{\partial f_2}{\partial t_{s2}} & \frac{\partial f_2}{\partial t_{s3}} & \frac{\partial f_2}{\partial t_{s4}} & \frac{\partial f_2}{\partial t_f} \\ \frac{\partial f_3}{\partial t_{s1}} & \frac{\partial f_3}{\partial t_{s2}} & \frac{\partial f_3}{\partial t_{s3}} & \frac{\partial f_3}{\partial t_{s4}} & \frac{\partial f_3}{\partial t_f} \\ \frac{\partial f_4}{\partial t_{s1}} & \frac{\partial f_4}{\partial t_{s2}} & \frac{\partial f_4}{\partial t_{s3}} & \frac{\partial f_4}{\partial t_{s4}} & \frac{\partial f_4}{\partial t_f} \\ \frac{\partial f_5}{\partial t_{s1}} & \frac{\partial f_5}{\partial t_{s2}} & \frac{\partial f_5}{\partial t_{s3}} & \frac{\partial f_5}{\partial t_{s4}} & \frac{\partial f_5}{\partial t_f} \end{bmatrix} \quad (22)$$

where f_i and g_i, $i = 1, \ldots, 5$, are the ith component of the vectors $\boldsymbol{f}$ and $\boldsymbol{g}$. The vector $\boldsymbol{g}$ is defined to be the unknown parameters that are to be corrected for during each iteration step, namely,

$$\boldsymbol{g} = [t_{s1} \quad t_{s2} \quad t_{s3} \quad t_{s4} \quad t_f]^T$$

The preceding Jacobian matrix can be calculated either analytically or numerically using, for example, finite difference.

5) Calculate the step direction

$$\boldsymbol{Del} = \left(\frac{\partial \boldsymbol{f}}{\partial \boldsymbol{g}}\right)^{-1} \cdot \boldsymbol{f} \quad (23)$$

6) Update the unknown variables using

$$\boldsymbol{g}_i = \boldsymbol{g}_i - \rho \times Del_i, \qquad i = 1, \ldots, 5 \quad (24)$$

where subscript i denotes the ith component and ρ is a constant representing the step size. As a general guide, the value of the constant ρ should be between zero and one to avoid divergence.

7) Repeat steps 2–6 until

$$\text{norm}(\boldsymbol{f}) \le \text{tolerance}$$

where norm refers to the Euclidean norm of the vector $\boldsymbol{f}$.

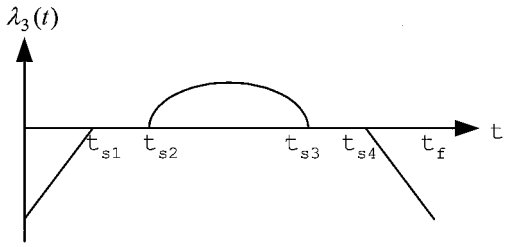

Fig. 2 Constrained time-optimal structure for the switching function $\lambda_3(t)$.

C. Calculation of the Costates

Once the optimal solution for the state variables and the control switch times are calculated, the corresponding optimal solution for the costates is computed next. A boundary-value problem involving the costates can be formulated with the help of the necessary conditions of optimality. From these conditions, one can infer the function form for the switching function $\lambda_3(t)$ as shown in Fig. 2.

Therefore, the boundary-value problem for the costates involves solving for the three unknowns, $\lambda_1(0)$, $\lambda_2(0)$, and $\lambda_3(0)$, given three interior conditions consisting of the transversality condition, Eq. (19) applied at the final time t_f, and the following two interior conditions, deduced from Fig. 2:

$$\lambda_3(t_{s1}) = 0, \qquad \lambda_3(t_{s3}) = 0 \tag{25}$$

The same numerical procedure outlined in Sec. IV.B can be used to solve for the costates by replacing the vectors $\boldsymbol{g}$ and $\boldsymbol{f}$ with the corresponding vectors of unknowns and errors, respectively.

V. Time-Optimal Control Design for the Rigid-Body Mode with a Second Time-Derivative Constraint

In this section, we formulate and solve a time-optimal control problem for the rigid-body mode that results in a smoother control input $u(t)$ than the one computed in Sec. IV. A straightforward and simple idea would be to add, to the previous time-optimal control problem, an additional constraint that limits the second time derivative of the control input $u(t)$. Consequently, we consider the following time-optimal control problem: Determine the control input $u(t)$ that minimizes

$$J = \int_0^{tf} \mathrm{d}t = t_f \tag{7}$$

subject to the following equations, constraints, and conditions:

1) State equations

$$\dot{\theta}_1 = \theta_2, \qquad \dot{\theta}_2 = \phi_0 u, \qquad \dot{u} = u_d, \qquad \dot{u}_d = u_{dd} \tag{26}$$

Note here that we have added an additional state variable equation, the last equation in Eqs. (26), which describes the second time derivative of the control input $u(t)$.

2) State constraints

$$S_1 = u - u_{\max} \le 0, \qquad S_2 = -u - u_{\max} \le 0 \tag{10}$$

3) Control constraints

$$u_{dd} - (u_{dd})_{\max} \le 0, \qquad -u_{dd} - (u_{dd})_{\max} \le 0 \tag{27}$$

4) Boundary conditions

$$\theta_1(0) = 0, \qquad \theta_1(t_f) = \theta_f, \qquad \theta_2(0) = 0$$
$$\theta_2(t_f) = 0, \qquad u(0) = 0, \qquad u(t_f) = 0$$
$$u_d(0) = 0, \qquad u_d(t_f) = 0 \tag{28}$$

Once again, we consider, in this problem, $u(t)$ and $u_d(t)$ as additional states and $u_{dd}(t)$ as the control input.

A. Necessary Conditions of Optimality

Following Jacobson et al.,[18] the necessary conditions of optimality can be derived by defining first the Hamiltonian H as

$$H = 1 + \lambda_1\dot{\theta}_1 + \lambda_2\dot{\theta}_2 + \lambda_3\dot{u} + \lambda_4\dot{u}_d + \eta_1(u - u_{\max})$$
$$+ \eta_2(-u - u_{\max}) = 1 + \lambda_1\theta_2 + \lambda_2\phi_0 u + \lambda_3 u_d + \lambda_4 u_{dd}$$
$$+ \eta_1(u - u_{\max}) + \eta_2(-u - u_{\max}) \tag{29}$$

Then, the necessary conditions of optimality require the following equations to be satisfied:

1) The state equations, given by Eqs. (26).

2) The costate equations, derived from

$$\dot{\lambda}_1 = -\frac{\partial H}{\partial \theta_1} \Rightarrow \dot{\lambda}_1 = 0, \qquad \dot{\lambda}_2 = -\frac{\partial H}{\partial \theta_2} \Rightarrow \dot{\lambda}_2 = -\lambda_1$$
$$\dot{\lambda}_3 = -\frac{\partial H}{\partial u} \Rightarrow \dot{\lambda}_3 = -\phi_0\lambda_2 - \eta_1 + \eta_2$$
$$\dot{\lambda}_4 = -\frac{\partial H}{\partial u_d} \Rightarrow \dot{\lambda}_4 = -\lambda_3 \tag{30}$$

where the multiplier functions $\eta_1(t)$ and $\eta_2(t)$ satisfy Eqs. (15)

3) The time-optimal control $u^*_{dd}(t)$.

a) For interior arc ($u - u_{\max} < 0$ and $-u - u_{\max} < 0$),

$$u^*_{dd}(t) = -(u_{dd})_{\max}\,\mathrm{sign}\left(\frac{\partial H}{\partial u_{dd}}\right)$$
$$\Rightarrow u^*_{dd}(t) = -(u_{dd})_{\max}\,\mathrm{sign}(\lambda_4(t)) \tag{31}$$

Therefore, the costate variable $\lambda_4(t)$ is the switching function.

b) For boundary arc ($u - u_{\max} = 0$ or $-u - u_{\max} = 0$),

$$\ddot{S}_i = 0, \qquad i = 1, \ldots, 2$$
$$\Rightarrow \ddot{u}(t) = 0 \Rightarrow \dot{u}_d(t) = 0 \Rightarrow u^*_{dd}(t) = 0 \tag{32}$$
$$\frac{\partial H}{\partial u_{dd}} = 0 \Rightarrow \lambda_4(t) = 0 \tag{33}$$

Note that the order of the state constraints, in this case, is two, that is, $p = 2$.

4) The transversality condition, given by Eq. (19).

5) The boundary conditions, given by Eqs. (28).

6) The costates $\lambda_1(t)$, $\lambda_2(t)$, and $\lambda_4(t)$ are continuous functions of time, whereas $\lambda_3(t)$, which is the costate associated with the state constraints [Eqs. (10)], becomes discontinuous at times of transitions between interior and boundary arcs and vice versa.

The time-optimal control structure for this problem can be deduced by first solving it without imposing the state constraints [Eqs. (10)]. Then, the resulting time-optimal control problem with only control constraints will have a control structure $u_{dd}(t)$ with at most three switches.

Therefore, one can guess the time-optimal structure for $u_{dd}(t)$ and $u(t)$ in the presence of the constraints [Eqs. (10)] to be as shown in Fig. 3.

Consequently, the solution, for the constrained time-optimal control problem, in state space consists of solving the boundary-value problem with the 12 variables θ_1, θ_2, u_d, u_{dd}, t_{s1}, t_{s2}, t_{s3}, t_{s4}, t_{s5}, t_{s6}, t_{s7}, and t_f. On the other hand, we have the eight boundary conditions [Eqs. (28)], plus the following four interior conditions, deduced from Fig. 3:

$$u(t_{s2}) = u_{\max}, \qquad u(t_{s5}) = -u_{\max}$$
$$u_d(t_{s2}) = 0, \qquad u_d(t_{s5}) = 0 \tag{34}$$

This boundary-value problem can be solved using the shooting method by applying the numerical procedure outlined in Sec. IV.B with appropriate modifications.

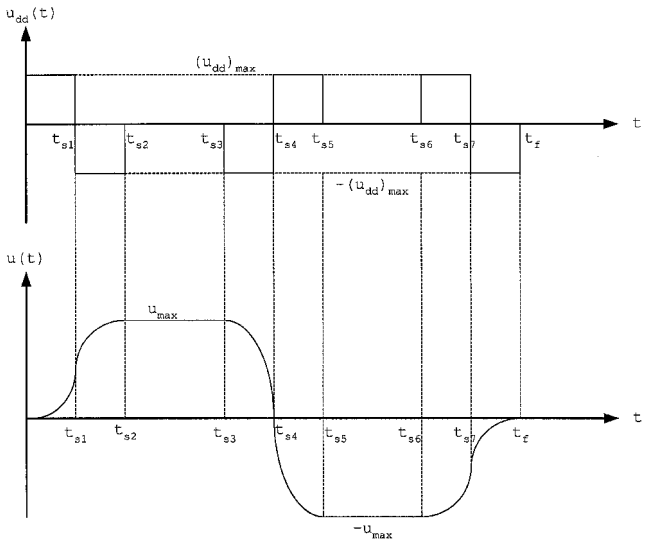

Fig. 3 Constrained time-optimal structure for $u_{dd}(t)$ and $u(t)$.

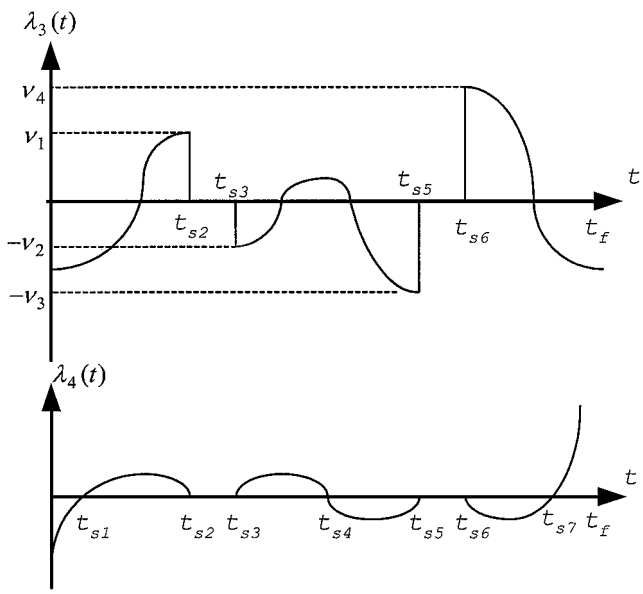

Fig. 4 Time-optimal structure for $\lambda_3(t)$ and $\lambda_4(t)$.

B. Calculation of the Costates

Once the optimal solution for the states is calculated, a boundary-value problem involving only the costates is formed and solved next. The main difficulty, in this case as opposed to the costates in Sec. IV.C, is that the costate associated with the state constraints $\lambda_3(t)$ is now discontinuous and satisfies[18]

$$\lambda_3\left(t_{s2}^+\right) = \lambda_3\left(t_{s2}^-\right) - \nu_1, \qquad \lambda_3\left(t_{s3}^+\right) = \lambda_3\left(t_{s3}^-\right) - \nu_2$$

$$\lambda_3\left(t_{s5}^+\right) = \lambda_3\left(t_{s5}^-\right) + \nu_3, \qquad \lambda_3\left(t_{s6}^+\right) = \lambda_3\left(t_{s6}^-\right) + \nu_4 \quad (35)$$

where $\nu_i > 0, i = 1, \ldots, 4$ are unknown function discontinuities for the costate $\lambda_3(t)$.

Based on the necessary conditions of optimality, the time-optimal structure, for $\lambda_3(t)$ and $\lambda_4(t)$ are as shown in Fig. 4. Consequently, the boundary-value problem for the costates involves the eight unknowns

$$\lambda_1(0),\ \lambda_2(0),\ \lambda_3(0),\ \lambda_4(0),\ \nu_1,\ \nu_2,\ \nu_3,\ \nu_4 \quad (36)$$

and the following eight boundary and interior conditions: 1) one transversality condition applied at either the initial or final time,

$$\lambda_4(0) = -[1/(u_{dd})_{\max}] \quad (37)$$

2) five switching conditions,

$$\lambda_4(t_{s1}) = 0, \qquad \lambda_4(t_{s2}) = 0, \qquad \lambda_4(t_{s4}) = 0$$

$$\lambda_4(t_{s5}) = 0, \qquad \lambda_4(t_7) = 0 \quad (38)$$

and 3) two conditions, which are the second and third of Eqs. (35), and equal to zeros because of λ_3 structure shown in Fig. 4:

$$\lambda_3\left(t_{s2}^+\right) = \lambda_3\left(t_{s2}^-\right) - \nu_1 = 0, \qquad \lambda_3\left(t_{s5}^+\right) = \lambda_3\left(t_{s5}^-\right) + \nu_3 = 0 \quad (39)$$

C. Calculation Algorithm

The numerical procedure for calculating the costates is illustrated in the following steps:

1) Assume starting values for the unknowns given in Eqs. (36).

2) Evaluate the vector of boundary and interior conditions given by

$$\boldsymbol{f} = \left[\lambda_4(t_{s1}) \quad \lambda_4(t_{s2}) \quad \lambda_4(t_{s4}) \quad \lambda_4(t_{s5}) \quad \lambda_4(t_{s7}) \quad \lambda_3\left(t_{s2}^+\right) \quad \lambda_3\left(t_{s5}^+\right)\right]^T$$

by integrating the proper costate equations

$$\dot{\boldsymbol{\lambda}} = A_i \lambda, \qquad i = 1, 2 \quad (40)$$

where the matrix A_1 is defined by

$$A_1 = \begin{bmatrix} 0 & 0 & 0 & 0 \\ -1 & 0 & 0 & 0 \\ 0 & -\phi_0 & 0 & 0 \\ 0 & 0 & -1 & 0 \end{bmatrix} \quad (41a)$$

and is valid for the time intervals $0 \le t \le t_{s2}^-$, $t_{s3}^+ \le t \le t_{s5}^-$, and $t_{s6}^+ \le t \le t_f$, whereas the matrix A_2 is defined by

$$A_2 = \begin{bmatrix} 0 & 0 & 0 & 0 \\ -1 & 0 & 0 & 0 \\ 0 & 0 & 0 & 0 \\ 0 & 0 & 0 & 0 \end{bmatrix} \quad (41b)$$

and is valid for the time intervals $t_{s2}^+ \le t \le t_{s3}^-$ and $t_{s5}^+ \le t \le t_{s6}^-$.

3) Evaluate the Jacobian matrix $\partial \boldsymbol{f}/\partial \boldsymbol{g}$, either analytically or numerically, where the vector $\boldsymbol{g}$ is the vector of unknowns defined as

$$\boldsymbol{g} = [\lambda_1(0) \quad \lambda_2(0) \quad \lambda_3(0) \quad \lambda_4(0) \quad \nu_1 \quad \nu_2 \quad \nu_3 \quad \nu_4]^T$$

4) Update the components of the vector $\boldsymbol{g}$ using Eqs. (23) and (24).

5) Repeat steps 2–4 until

$$\text{norm}(\boldsymbol{f}) \le \text{tolerance}$$

Finally, the multiplier functions $\eta_1(t)$ and $\eta_2(t)$ are obtained from the following:

$$\eta_1(t) = \begin{cases} -\phi_0 \lambda_2(t), & t_{s2}^+ \le t \le t_{s3}^- \\ 0, & \text{elsewhere} \end{cases} \quad (42)$$

$$\eta_2(t) = \begin{cases} \phi_0 \lambda_2(t), & t_{s5}^+ \le t \le t_{s6}^- \\ 0, & \text{elsewhere} \end{cases} \quad (43)$$

VI. Numerical Example

As an example to illustrate the numerical procedure and show the effectiveness of the proposed design method, we consider the time-optimal single-axis maneuver problem for a flexible system consisting of a rigid hub with two uniform elastic appendages attached to it, as shown in Fig. 5. A single actuator that exerts an external torque $u(t)$ on the rigid hub controls the motion of the system. The objective is to design a control input $u(t)$ that can perform a rest-to-rest maneuver through a desired angular displacement as quickly and accurately as possible.

Table 1 System dimensions, appendage materials, and maneuver specifications

Parameter	Value
Radius of the rigid central hub r	1.00 m
Length of one appendage L	40.00 m
Appendage material stiffness EI	1500.00 N · m^2
Appendage material density ρ	0.04096 kg/m
Mass of the rigid central hub	400.00 kg
Maximum torque available u	150.00 N · m
Command slew angle x_{1f}	90.00 deg
Total rotational inertia J^*	2081.97547 kg · m^2

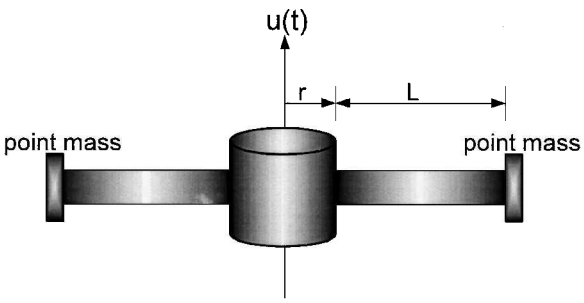

Fig. 5 Flexible structure.

For comparison purposes, we use the same material and maneuver specifications that are used in Ref. 4 for a relatively large structure. The system dimensions, appendage material, and maneuver specifications are shown in Table 1.

The Euler–Bernouli beam assumption is made to obtain the equations of motion for the system. It is assumed further that the beam is inextensible, in the sense that the stretch of the neutral axis is negligible, and no structural damping is present. Furthermore, the gyroscopic effects are assumed to be small and are neglected.

The assumed mode method[19] based on modal expansion is applied to the rigid hub with two flexible appendages, where the rigid body mode and the first 10 vibrational modes are retained in the evaluation model. The normalized mode shapes for a fixed–free cantilever beam are used as the assumed mode shapes. The discretized equations of motion, in matrix form, are

$$M\ddot{\boldsymbol{x}} + K\boldsymbol{x} = \boldsymbol{b}u \tag{44}$$

where $\boldsymbol{x}$ and $\boldsymbol{b}$ are 11×1 vectors representing the state and input distribution vectors and M and K are 11×11 matrices representing the mass and stiffness matrices, respectively. The boundary conditions for a 90 deg rest-to-rest maneuver are

$$\boldsymbol{x}(0) = [0 \quad 0 \quad \cdots \quad 0]^T, \qquad \boldsymbol{x}(t_f) = [\pi/2 \quad 0 \quad \cdots \quad 0]^T \tag{45}$$

Using the matrix of eigenvectors, normalized with respect to the mass matrix, the system in Eq. (44) is transformed to

$$\ddot{\boldsymbol{q}} + \Lambda\boldsymbol{q} = \beta u \tag{46}$$

using the transformation

$$\boldsymbol{x} = \Phi\boldsymbol{q} \tag{47}$$

where $\boldsymbol{x}$ and $\boldsymbol{q}$ are the position vectors in physical and modal coordinates, respectively, Λ is an 11×11 diagonal matrix with the diagonals being ω_i^2, $i = 0, \ldots, 10$, and Φ is an 11×11 matrix of eigenvectors. Table 2 shows the natural frequencies ω_i, in radian per second, and the components of the vector β in Eqs. (46).

The three control inputs, namely, the bang–bang, the bang–bang with first time-derivative constraints, and the bang–bang with second time-derivative constraints, are calculated according to the numerical procedures presented in Secs. III–V, respectively, for only the rigid-body mode, the first equation in Eqs. (46). It is written in state space as

$$\dot{z}_1 = z_2, \qquad \dot{z}_2 = 0.0219u \tag{48}$$

where $z_1 = \boldsymbol{q}_0 = \theta$ and $z_2 = \dot{\boldsymbol{q}}_0 = \dot{\theta}$.

Table 2 Modal quantities

i	ω_i	β_i
0	0	0.0219
1	1.1507	0.0543
2	3.0098	−0.0353
3	7.5342	−0.0143
4	14.5654	−0.0077
5	24.0232	−0.0049
6	35.8722	−0.0034
7	50.2238	−0.0026
8	66.8855	−0.0020
9	86.6068	−0.0015
10	108.1406	−0.0013

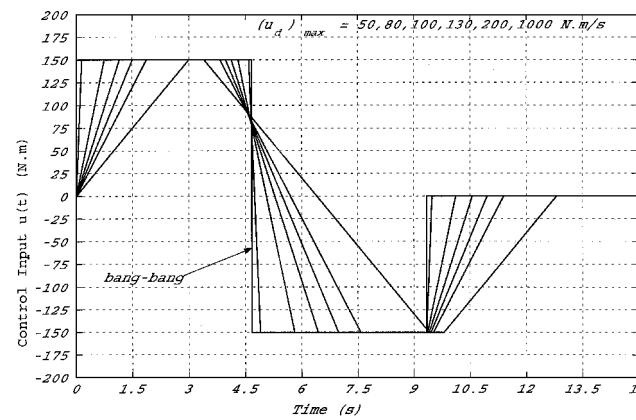

Fig. 6 Control input approaching bang–bang when first time derivative approaches infinity.

The boundary conditions are transformed from physical to modal coordinates using Eq. (47) to give

$$\boldsymbol{z}(0) = \begin{bmatrix} 0 \\ 0 \end{bmatrix}, \qquad \boldsymbol{z}(t_f) = \begin{bmatrix} 71.6733 \\ 0 \end{bmatrix} \tag{49}$$

Because the maximum torque input available (from Table 1) is equal to 150 N · m, the value of $u_{\max}$ is set to 150 N · m. The maximum first time derivative $(u_d)_{\max}$ and maximum second time derivative $(u_{dd})_{\max}$ for the torque input are given the values 100 N · m/s and 50 N · m/s^2, respectively. Obviously, these values are user defined and directly control the smoothness of the computed control input $u(t)$. The selected values for $(u_d)_{\max}$ and $(u_{dd})_{\max}$ give approximately the minimum postmaneuver energy, thereby achieving precise pointing accuracy. Furthermore, when the values of $(u_d)_{\max}$ and $(u_{dd})_{\max}$ approach infinity, the resulting control inputs $u(t)$ approach the bang–bang control input for the rigid-body mode. This is illustrated in Figs. 6 and 7 and provides an additional proof of the optimality of the computed control inputs with time-derivative constraints.

The numerical algorithms, outlined in Secs. III–V are programmed in MATLAB®[20] in an IBM-compatible personal computer with a 750-MHz Pentium III processor. The resulting switching times, in seconds, for $u(t)$, $u_d(t)$, and $u_{dd}(t)$ are shown in Table 3. The computer execution time for the calculation of the switching times for the control input with first time-derivative constraints is less than that required for the control input with second time-derivative constraints because the latter involves more variables than the former control input. The initial values for the switching times, in seconds, are assigned the values $t_{s1} = 1$, $t_{s2} = 2$, $t_{s3} = 3$, $t_{s4} = 4$, and $t_f = 5$ for the first time derivative and $t_{s1} = 1$, $t_{s2} = 2$, $t_{s3} = 3$, $t_{s4} = 4$, $t_{s5} = 5$, $t_{s6} = 6$, $t_{s7} = 7$, and $t_f = 8$ for the second time derivative. Furthermore, analytical derivatives were used to calculate the Jacobian matrix. The switching times for the control input with first and second time-derivative constraints were calculated in 0.11 and 0.33 s, respectively.

Note that no other control input $u(t)$ capable of exerting a maximum torque of $u_{\max}$ is able to perform a faster maneuver than

Table 3 Switching times

Bang–bang control	Control with first time-derivative limit	Control with second time-derivative limit
$t_{s1} = 4.6693$	$t_{s1} = 1.5000$	$t_{s1} = 1.7321$
$t_f = 9.3386$	$t_{s2} = 3.9792$	$t_{s2} = 3.4641$
——	$t_{s3} = 6.9792$	$t_{s3} = 4.0051$
——	$t_{s4} = 9.4583$	$t_{s4} = 6.4546$
——	$t_f = 10.9583$	$t_{s5} = 8.9041$
——	——	$t_{s6} = 9.4451$
——	——	$t_{s7} = 11.1771$
——	——	$t_f = 12.9092$

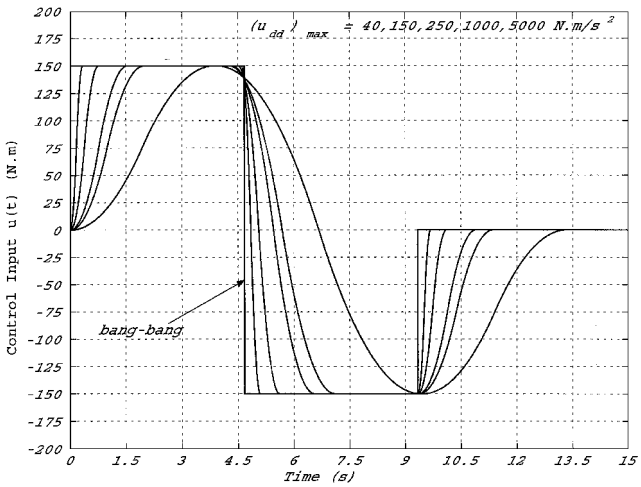

Fig. 7 Control input approaching bang–bang when second time derivative approaches infinity.

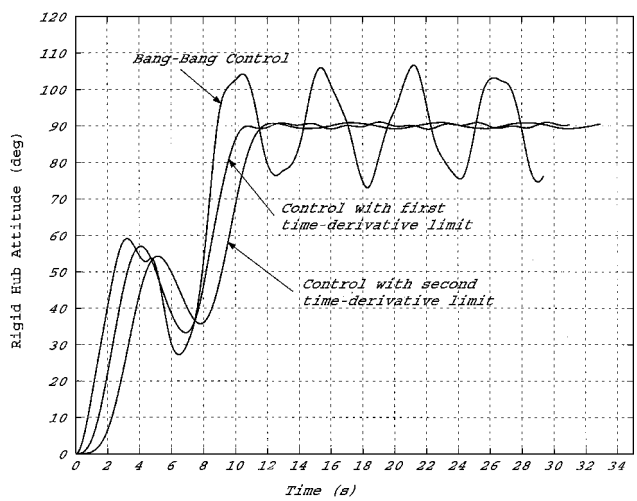

Fig. 8 Rigid-hub attitudes.

the bang–bang control input $u(t)$ for the rigid-body mode. Consequently, the maneuver time resulting from the bang–bang control input serves as a basis for comparison for the maneuver times resulting from the other control inputs.

The three control inputs $u(t)$ result in the rigid-hub attitudes shown in Fig. 8. The bang–bang control input, as noted in Ref 4, is antisymmetric about the midmaneuver time $(t_f/2)$. Similarly, the control inputs with first and second time-derivative constraints have also preserved the anti-symmetry property of the rigid-body control input and can be utilized to reduce the number of unknown variables. The energy of the system E during and after the maneuver has been calculated using

$$E = \tfrac{1}{2}\dot{\boldsymbol{x}}^T M\dot{\boldsymbol{x}} + \tfrac{1}{2}\boldsymbol{x}^T K\boldsymbol{x} \tag{50}$$

and is shown in Fig. 9 for the three control inputs.

It is seen that when the bang–bang control input is applied to the flexible system, the rigid hub would continue to oscillate

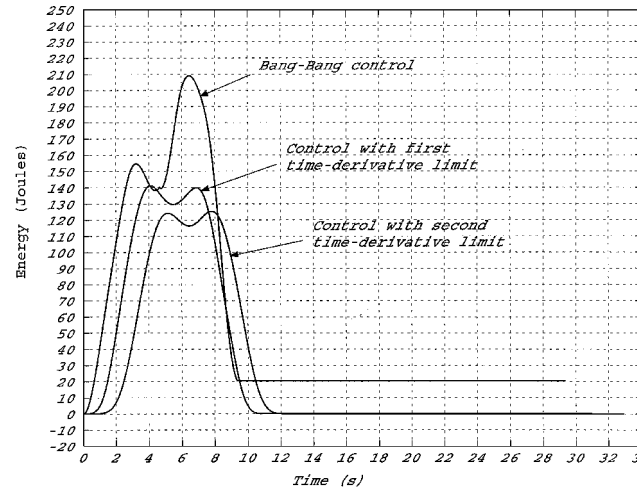

Fig. 9 Energy during and after a maneuver.

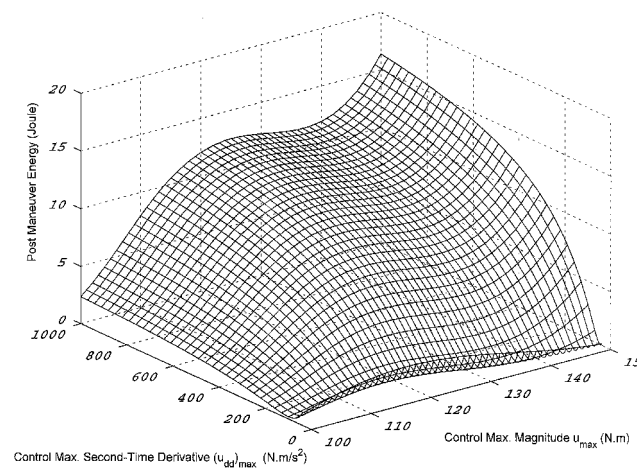

Fig. 10 Effect of varying maximum control magnitude and maximum control second time derivative on postmaneuver energy.

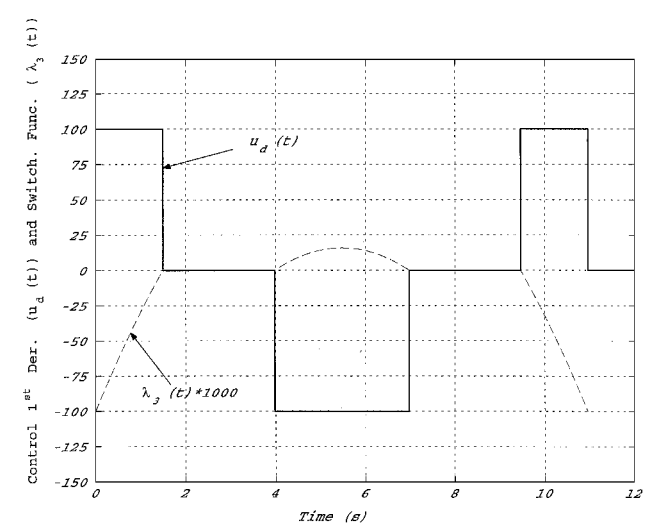

Fig. 11 Control with first time-derivative constraint and its switching function.

after the maneuver has been completed. This is due to the energy spillover to the flexible modes resulting in a rigid-hub pointing error. However, as evident from Fig. 8, the smooth control inputs, while achieving near minimum-time maneuvers, nearly eliminated the energy spillover to the flexible modes, thus, achieving precise pointing accuracy. As a result of smoothing the bang–bang control input, the residual energy when applying the first and second time-derivative limit control inputs has been reduced by 98.87 and

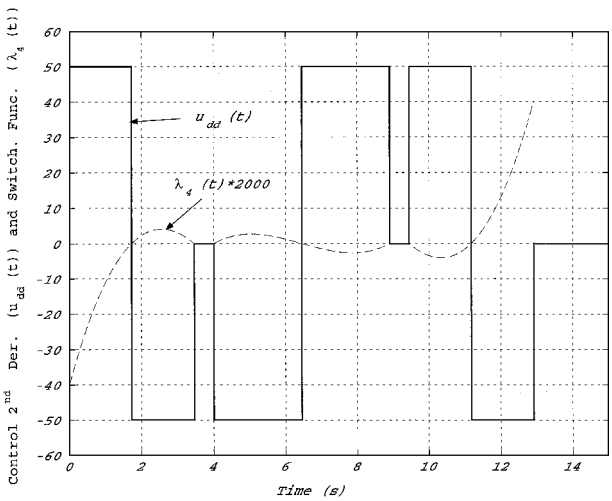

Fig. 12 Control with second time-derivative constraint and its switching function.

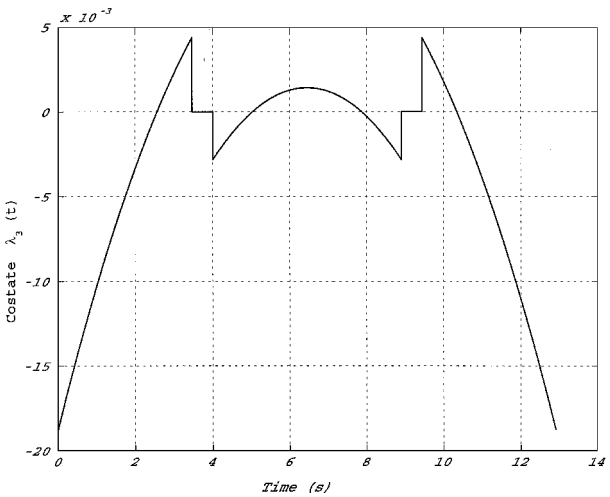

Fig. 13 Discontinuous costate λ_3.

99.76%, respectively. The maneuver time compared with that resulting from the application of the bang–bang control input for the rigid-body mode has increased by 17.34 and 38.23% when applying the first and second time-derivative limit control inputs, respectively.

The effect of changing both the maximum control magnitude $u_{\max}$ as well as the maximum second time-derivative $(\mathrm{d}^2u/\mathrm{d}t^2)_{\max}$ on the postmaneuver energy is shown in Fig. 10. The general trend in Fig. 10 is that, for a given maximum control magnitude, the postmaneuver energy increases as the maximum second time derivative increases. The rate at which the postmaneuver energy increases is also seen to increase as the maximum control magnitude is increased. Similarly, for a given maximum second time-derivative, the postmaneuver energy increases when the maximum control magnitude is increased.

The switching functions associated with the time-derivative constrained optimal control problems are shown in Figs. 11 and 12 for the first and second time-derivative constraints, respectively. Because of its discontinuous nature, the costate $\lambda_3(t)$ associated with the state constraints for the case of second time-derivative limit is shown in Fig. 13.

VII. Conclusions

We outlined a new control design procedure to perform a near-minimum-time maneuver for flexible structures. The basic idea is to smooth the bang–bang time-optimal control input, designed for the rigid-body mode, and apply it to the flexible system. This is achieved through formulating and solving the time-optimal control problem for the rigid-body mode with the addition of a constraint that limits the first time derivative of the control input. A smoother control input is also calculated through constraining the second time derivative. The resulting time-optimal control problems contain both control and state constraints. Then the necessary conditions of optimality are derived, which lead to forming a boundary-value problem. We formulate a boundary-value problem that contains only the state variable, thereby reducing the numerical complexity of the problem. A simple numerical algorithm, based on the shooting method, is outlined to solve the resulting boundary-value problem. The validity of the proposed technique is proved through a numerical example, whereby it is desired to minimize both the maneuver time and the free vibration occurring at the end of the maneuver, for a flexible structure consisting of a rigid hub with flexible appendages. The numerical simulation for the three types of control inputs has shown that smoothing the bang–bang control input almost eliminates the residual energy at the expense of slight increase in maneuver time. The control input with first time-derivative constraints is seen to be superior to the control input with second time-derivative constraints because the former involves a fewer number of variables, results in less maneuver time, and provides good vibration suppression.

References

[1]Singh, T., and Vadali, S., "Robust Time-Optimal Control: Frequency Domain Approach," *Journal of Guidance, Control, and Dynamics*, Vol. 17, No. 2, 1994, pp. 346–353.

[2]Ben-Asher, J., Burns, J., and Cliff, E., "Time-Optimal Slewing of Flexible Spacecraft," *Journal of Guidance, Control, and Dynamics*, Vol. 15, No. 2, 1992, pp. 360–367.

[3]Liu, Q., and Wie, B., "Robust Time-Optimal Control of Uncertain Flexible Spacecraft," *Journal of Guidance, Control, and Dynamics*, Vol. 15, No. 3, 1992, pp. 597–604.

[4]Singh, G., Kabamba, P., and McClamroch, N., "Planar, Time-Optimal, Rest-to-Rest Slewing Maneuvers of Flexible Spacecraft," *Journal of Guidance, Control, and Dynamics*, Vol. 12, No. 1, 1989, pp. 71–81.

[5]Pao, L., "Minimum-Time Control Characteristics of Flexible Structures," *Journal of Guidance, Control, and Dynamics*, Vol. 19, No. 1, 1996, pp. 123–129.

[6]Meier, E., and Bryson, A., "An Efficient Algorithm for Time-Optimal Control of a Two-Link Manipulator," *Journal of Guidance, Control, and Dynamics*, Vol. 13, No. 5, 1990, pp. 859–866.

[7]Ryan, E., *Optimal Relay and Saturating Control System Synthesis*, Peter Peregrinus, London, 1982, pp. 101–103.

[8]Barbieri, E., and Ozguner, U., "A New Minimum-Time Control Law for a One-Mode Model of a Flexible Slewing Structure," *IEEE Transactions on Automatic Control*, Vol. 38, No. 1, 1993, pp. 142–146.

[9]Scrivener, S., and Thompson, R., "Survey of Time-Optimal Attitude Maneuvers," *Journal of Guidance, Control, and Dynamics*, Vol. 17, No. 2, 1994, pp. 225–233.

[10]Junkins, J., Rahman, Z., and Bang, H., "Near-Minimum-Time Control of Distributed Parameter Systems: Analytical and Experimental Results," *Journal of Guidance, Control, and Dynamics*, Vol. 14, No. 2, 1991, pp. 406–415.

[11]Hecht, N., and Junkins, J., "Near-Minimum-Time Control of a Flexible Manipulator," *Journal of Guidance, Control, and Dynamics*, Vol. 15, No. 2, 1992, pp. 477–481.

[12]Sage, A. P., and White, C. C., *Optimum Systems Control*, Prentice–Hall, Upper Saddle River, NJ, 1977, pp. 103–106.

[13]Hamilton, W., "On Nonexistence of Boundary Arcs in Control Problems with Bounded State Variables," *IEEE Transactions on Automatic Control*, Vol. AC-17, No. 3, 1972, pp. 338–343.

[14]Maurer, H., "On Optimal Control Problems with Bounded State Variables and Control Appearing Linearly," *SIAM Journal of Control and Optimization*, Vol. 15, No. 3, 1977, pp. 345–362.

[15]Maurer, H., and Gillessen, W., "Application of Multiple Shooting to the Numerical Solution of Optimal Control Problems with Bounded State Variables," *Computing*, Vol. 15, 1975, pp. 105–126.

[16]Oberle, H., "Numerical Solution of Minimax Optimal Control Problems by Multiple Shooting Technique," *Journal of Optimization Theory and Applications*, Vol. 50, No. 2, 1986, pp. 331–357.

[17]Maurer, H., and Wiegand, M., "Numerical Solution of a Drug Displacement Problem with Bounded State Variables," *Optimal Control Applications and Methods*, Vol. 13, 1992, pp. 43–55.

[18]Jacobson, D., Lele, M., and Speyer, J., "New Necessary Conditions of Optimality for Control Problems with State-Variable Inequality Constraints," *Journal of Mathematical Analysis and Applications*, Vol. 35, 1971, pp. 255–284.

[19]Junkins, J., and Kim, Y., *Introduction to Dynamics and Control of Flexible Structures*, AIAA Education Series, AIAA, Washington, DC, 1993, pp. 185–196.

[20]"MATLAB User's Guide," MathWorks, Inc., Natick, MA, 1999.